Calorimetry

in

High-Energy Elementary-Particle Physics

Joint Dutch-Belgian-German Graduate School
Physikzentrum Bad Honnef
8-9 September 2006

Jim Crittenden
Laboratory for Elementary-Particle Physics
Cornell University

Calorimetry in Action

Deep-inelastic electron-proton scattering at HERA

$e + p \rightarrow e + \text{quark jet} + X$

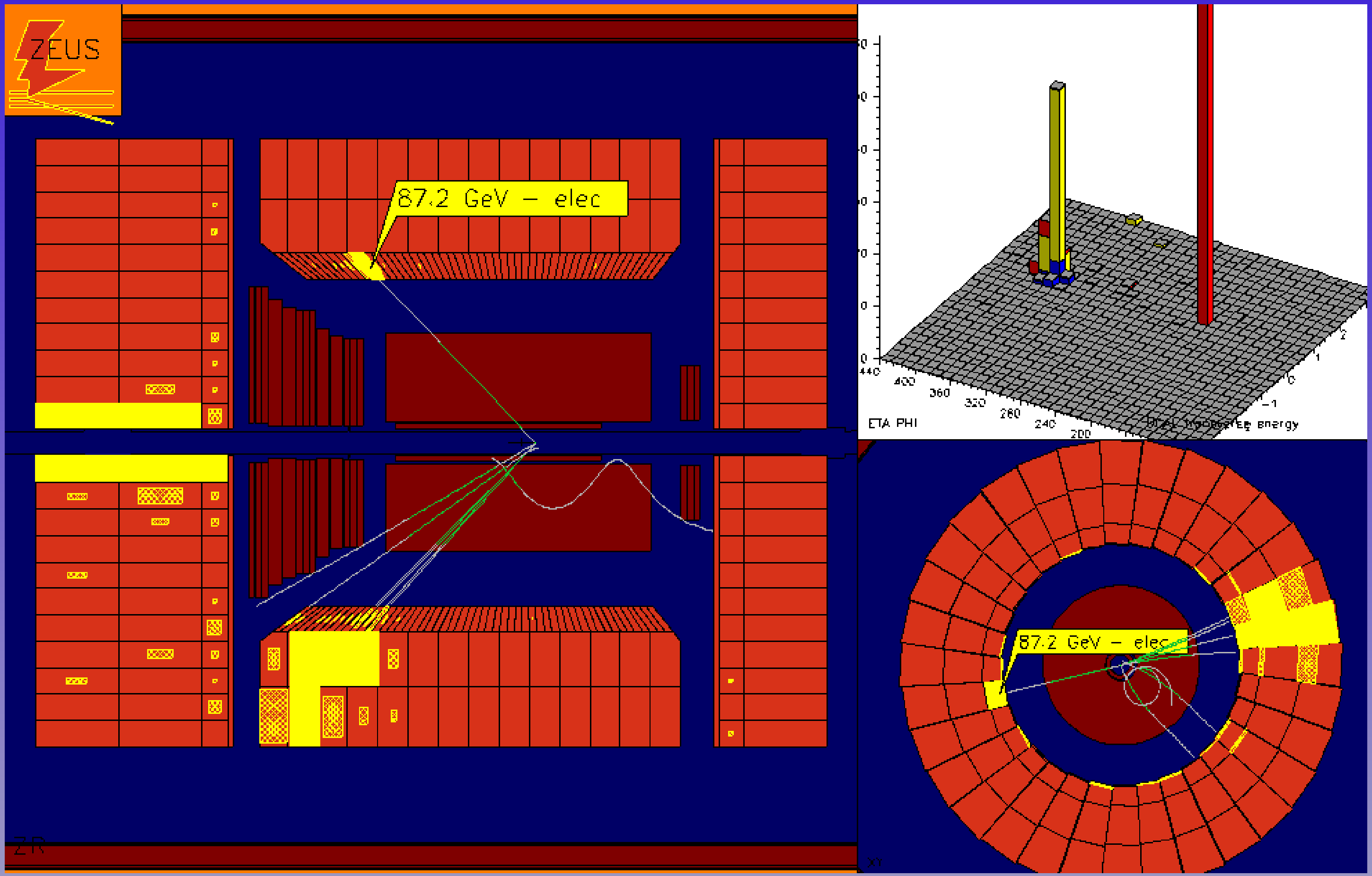

The ZEUS Uranium/Scintillator Calorimeter

Lecture Series Outline

I. Physical processes

- A. Multiple scattering
- B. Energy loss by electrons and positrons
  1. Ionization
  2. Bremsstrahlung
  3. Annihilation
- C. Interactions of photons
  1. Photo-electric effect
  2. Compton scattering
  3. Pair production
- D. Energy loss mechanisms for hadrons

II. Electromagnetic calorimeters

- A. Shower formation
- B. Scintillating Crystals
- C. Sampling Calorimeters
  1. Sampling fraction vs photostatistics
  2. Systematic limitations

III. Hadronic sampling calorimeters

- A. Shower development
  1. Leakage
  2. Time
- B. Energy loss mechanisms
- *C. Compensation*, e/h
  1. Role of neutrons
  2. Linearity & Resolution
- D. Precision limits

IV. Calibration techniques

- A. Test beam programs
- B. ZEUS uranium noise method
- C. Uniformity/intercalibration
- D. Guided ^{60}Co source monitoring
- E. Laser/LED monitoring (CMS)

Bibliography

I. **R. Wigmans**, *Energy Measurement in Particle Physics* (2000)

II. **P.B.Cushman**, *Electromagnetic and Hadronic Calorimeters* in *Instrumentation in High Energy Physics*, ed. F.Sauli (1992)

III. **C.Fabjan**, *Calorimetry in High-Energy Physics*, in *Experimental Techniques in High-Energy Physics*, ed. T.Ferbel (1987)

IV. **U.Amaldi**, *Calorimetry in High-Energy Physics*, in *Experimental Techniques in High-Energy Physics*, ed. T.Ferbel (1987)

V. **R.Fernow**, *Introduction to Experimental Particle Physics* (1986)

VI. **C. Grupen**, *Particle Detectors* (1996)

General Considerations

The essential concept of calorimetry is to measure the energy of final states via total absorption. The absorption is achieved via shower formation. The precision limit is determined by the ***statistics*** inherent in this physical process, thus scaling with $\sqrt{N}$, where N is the number of shower particles.

A further important aspect of shower formation is the logarithmic energy scaling of the penetration depth of the shower, and attendant consequences for detector size.

These considerations lead to the following comparisons with magnetic tracking measurements:

I. Calorimetric energy measurements of sufficient precision are possible up to several hundred GeV. Amazing dynamic range can be achieved (ZEUS: $1/10^5$, L3: $1/10^7$)

II. Relative measurement precision scales for magnetic tracking as $\sigma/E \propto E$ and for calorimetry as $\sigma/E \propto 1/\sqrt{E}$. Examples of crossover points are ZEUS: 20 GeV and ALEPH: 45 GeV.

III. Necessary detector volumes scale only logarithmically for calorimeters, in many cases making them the only feasible alternative in terms of cost/engineering effort.

Part I: Physical Processes

I. Multiple scattering

II. Energy loss mechanisms for electrons and positrons

A. Ionization

B. Bremsstrahlung

C. Annihilation

III. Energy loss mechanisms for photons

A. Photo-electric effect

B. Compton scattering

C. Pair production

IV. Energy loss mechanisms for hadrons

A. Ionization

B. Nuclear interactions

C. Elastic scattering (e.g. neutrons)

D. Decays (μ, ν production)

Multiple Scattering

Serves our lectures as a transition from negligible perturbation of the particle trajectory to full absorption. Here we assume constant kinetic energy, i.e. elastic scattering. This process will turn out to be closely related to the transverse profile of electromagnetic showers.

Coulomb-scattering scales with the squared charges, so scattering in matter is dominated by scattering off nuclei (rather than off electrons) for *Z*>10. Scattering of spin 0 (Rutherford) and spin ½ (Mott) particles are identical in a small-angle approximation.

Quantum limits of range of integration over scattering angles determined by resolving atom but not nucleus. Result can be defined in terms of radiation length L_R, to be defined later.

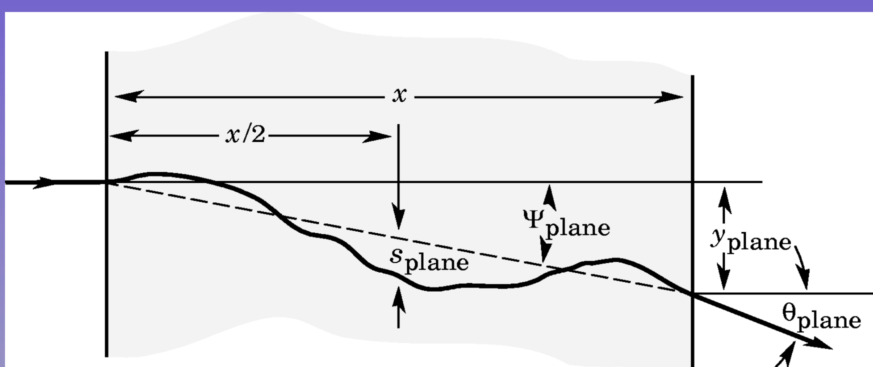

(ref: Fernow)

No dependence on mass of scattered

$$\Theta^{\text{rms}}_{\text{plane}} = \frac{1}{\sqrt{2}} \frac{21\text{MeV}}{\beta\, p\, c} q \sqrt{\frac{x}{L_{\text{R}}}} = 13 \text{ mrad}$$

$$Y^{\text{rms}}_{\text{plane}} = \frac{1}{\sqrt{3}} \Theta^{\text{rms}}_{\text{plane}}\, x = 1.3 \text{ cm}$$

Example: 20 GeV muon in ZEUS uranium calorimeter
L_R = 3.3 mm, x = 2.5 m ⇒ 0.7 Mb, $2\text{x}10^6$ scatters

Energy Loss via Ionization

Bethe-Bloch Formula

(ref: PDG)

$$-\frac{dE}{dx} \propto q^2 \frac{Z}{A} \frac{1}{\beta^2} \left[\frac{1}{2} \ln \frac{2 m_e c^2 \beta^2 \gamma^2 T_{\max}}{I^2} - \beta^2 - \frac{\delta(\beta\gamma)}{2} \right]$$

Early Fermi: 'counter-intuitive' β^{-2}

Bethe (1930): relativistic rise

Broad momentum range of 'Minimum Ionizing': 2 MeV/cm

Less loss for heavier elements

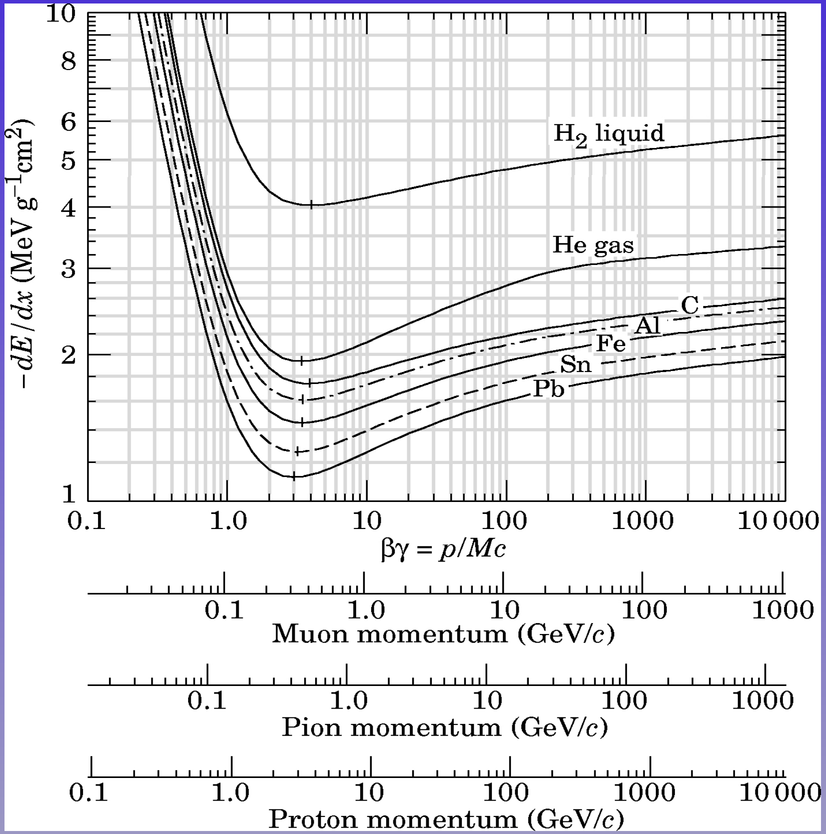

Bremsstrahlung

Radiation by an accelerated electron

$$\frac{\mathrm{d}E}{\mathrm{d}t} = \frac{2e^2}{3c^3} a^2$$

$\Rightarrow$ radiated power due to synchrotron radiation $\propto a^4 \propto B^4 \propto R^{-4}$!

Radiation by an accelerated charge *qe* in the field of a charge *Ze*

$$\frac{\mathrm{d}\sigma}{\mathrm{d}k} \simeq 5\,\alpha\,q^4 Z^2 \frac{e^4}{M\beta\,c^3}\,\frac{1}{k}\,\ln\frac{M\,\beta^2\,c^2\,\gamma^2}{k}$$

I. Scales with 1/M
   - 200 times larger for $e^{\pm}$ than $\mu^{\pm}$

II. Scales with Z^2
   - Brems off nucleus dominates
   - Ionization scales only with Z

III. Scales with 1/k: 'infrared divergence'

Mean angle of photon emission

$$< \theta_\gamma > = m_e c^2 / E$$

independent of photon energy

Energy Loss via Bremsstrahlung

Definition of Radiation Length

Calculating the energy loss, we define σ_{rad}:

$$\left.\boxed{\frac{\mathrm{d}E}{\mathrm{d}x}}\right|_{\mathrm{rad}} = \int_0^{k_{\max}} k\, n_a \frac{\mathrm{d}\sigma}{\mathrm{d}k}\,\mathrm{d}k = n_a\, \boxed{E_{\mathrm{init}}}\, \sigma_{\mathrm{rad}}$$

where

$$\sigma_{\mathrm{rad}} = \frac{1}{E_{\mathrm{init}}} \int_0^{k_{\max}} k \frac{\mathrm{d}\sigma}{\mathrm{d}k}\,\mathrm{d}k$$

Under the assumption of complete screening of the nuclear charge by the atomic electrons, the integral gives

$$\sigma_{\mathrm{rad}} = 4\,\sigma_0 \ln\left(183\, Z^{-1/3}\right)$$

$$\sigma_0 = \alpha\, Z^2 r_0^2 = \alpha\, Z^2 \times 80\ \mathrm{mb}$$

which is independent of the initial energy !

Since the energy loss is proportional to the initial energy, we can define a length characterizing the exponential decrease in energy:

$$1/L_R = 4\,\sigma_0\, n_a \ln(183\, Z^{-1/3})$$

(ref: Fernow)

Energy Loss Mechanisms for Electrons and Positrons in Lead

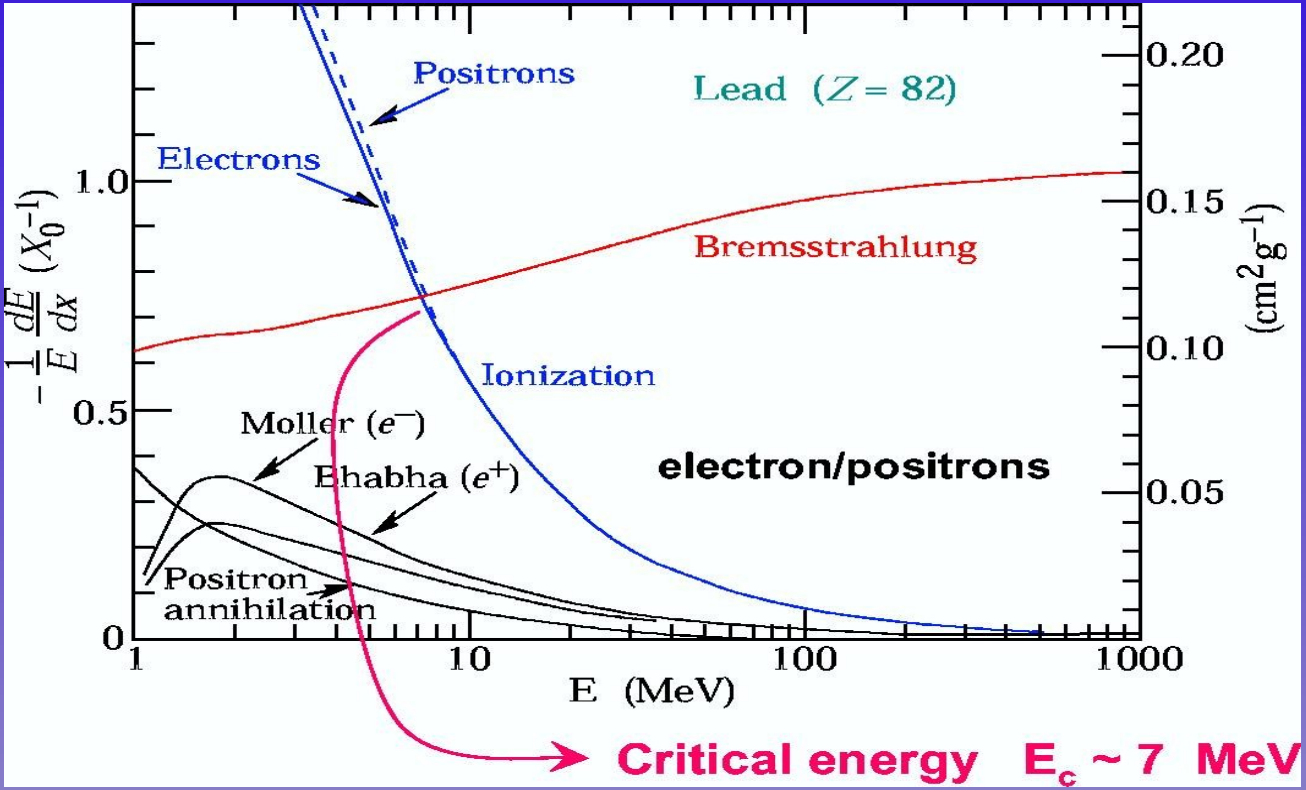

Rough Approximation: $E_{critical} \cong 550$ MeV / Z

Interactions of Photons with Matter

I. Photo-electric effect
- $E_\gamma \propto m_e c^2$
- $\sigma \propto Z^5$!

II. Compton Scattering

III. Pair-production
- Same physics as bremsstrahlung

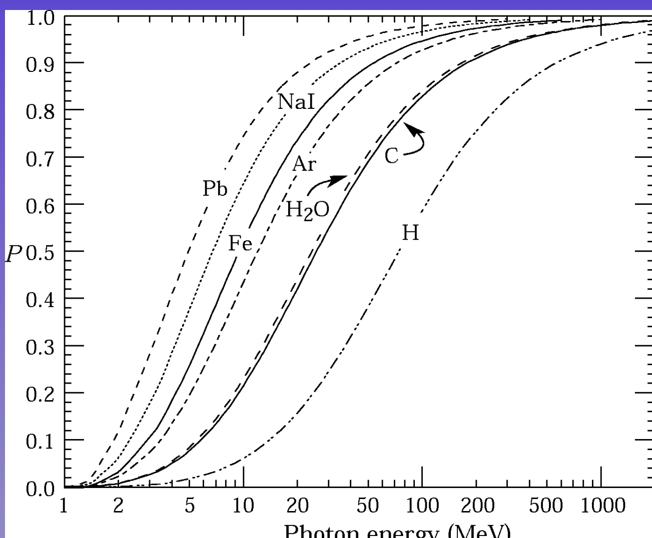

Low Energy:
Probability of pair-production vs Compton scattering

$$L_R^{\gamma} = 9/7\ L_r^{e}$$

NB: this is also the *interaction length* for photons

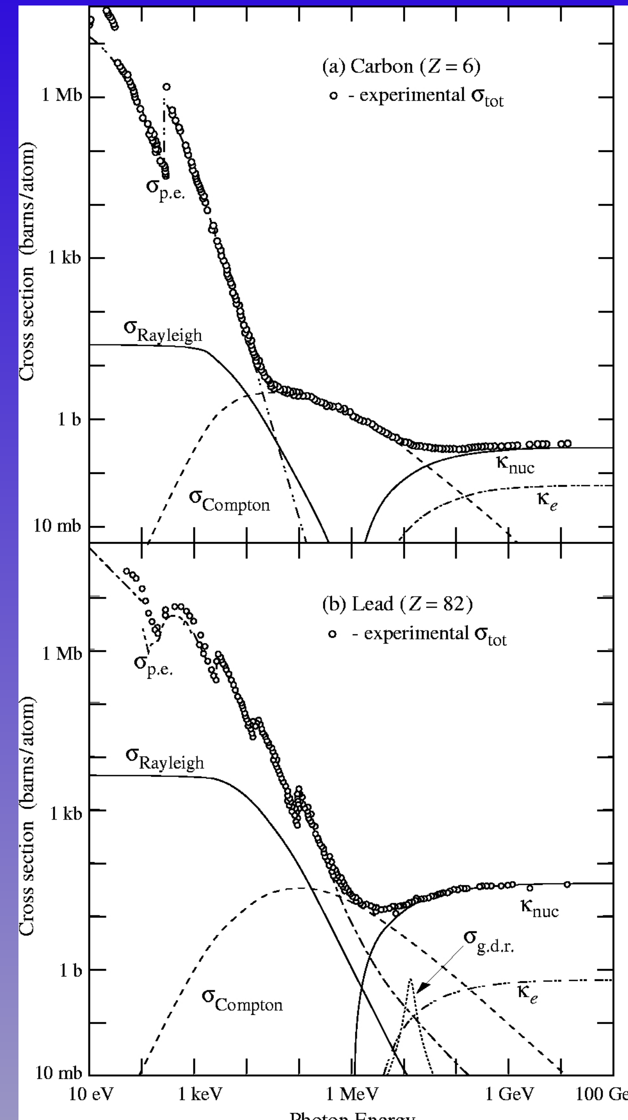

Electromagnetic Showers

Passive Material + Cloud Chamber

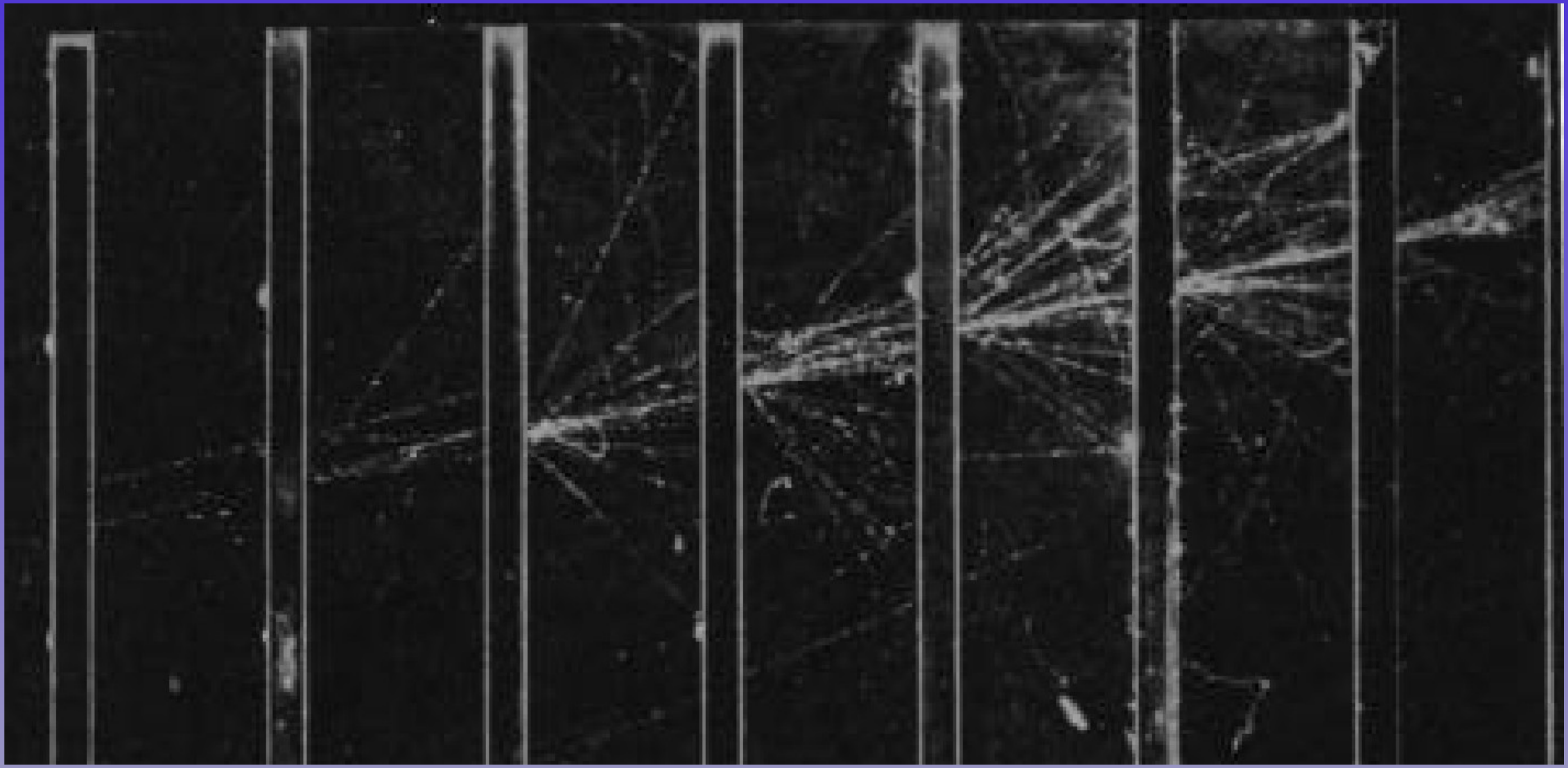

EM Calorimeter Design Parameters

(ref: Rossi,Amaldi)

- Critical Energy: $\epsilon \approx 550$ MeV/Z
- Radiation Length: X_0 [g/cm^2]= $\rho L_R \approx 180\ A/Z^2$
- Molière Radius: R_M [g/cm^2] $\approx X_0$ (21 MeV/ϵ) $\approx$ 7 A/Z

To calculate the visible signal from the shower, define the total track length in units of X_0: T.
T depends on the minimum detectable energy associated with the choice of active material: E_{min}
For E_{min}=0, all electrons and positrons are detected, and the signal T = E / ϵ, corresponding to a sensitivity factor F = 1. Calorimetry works when F is independent of E.

To get an estimate of the signal, Rossi made two assumptions: 1) the $e^{\pm}$ deposit an energy ϵ in each radiation length, and 2) the bremsstrahlung and pair-production processes occur according to their high-energy formulae. In this approximation, one obtains a reasonably accurate parameterization for many materials of the signal:

$$F(\xi) = e^{\xi}\left(1 + \xi \ln \frac{\xi}{1.53}\right)$$

with

$$\xi = 4.6 \frac{A}{Z} \frac{E_{\min}}{\epsilon}$$

For $E_{min} = \epsilon$,
F is about 30%.

Profiles of Electromagnetic Showers

Transverse

Containment radius

R(95%) ≅ 2 R_M

For example, a transverse cell size of 5 cm was chosen for the ZEUS uranium calorimeter, where R_M = 3 cm.

Longitudinal

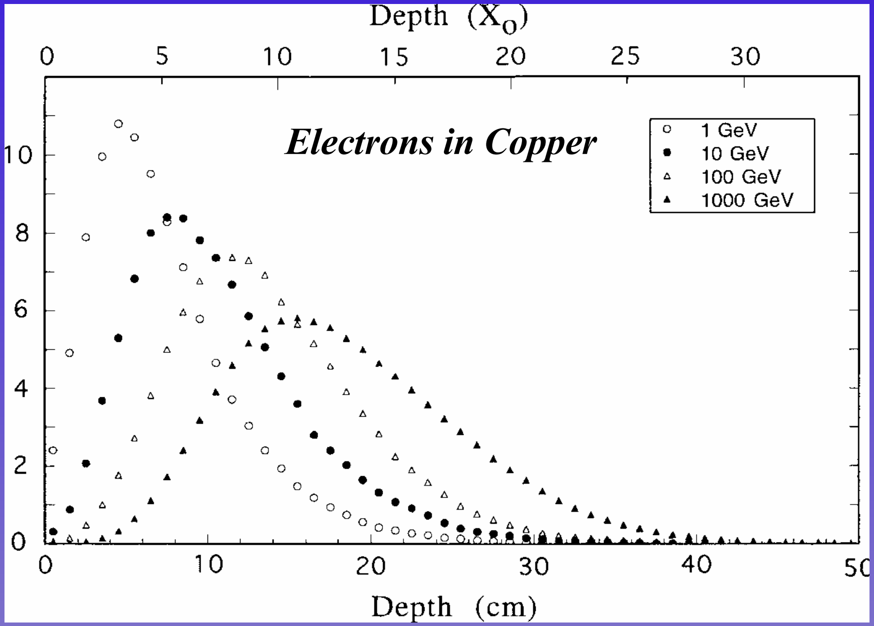

$$t_{\max} = \ln\frac{E}{\epsilon} - a, \quad t = x/X_0$$

$$e^{\pm}: a = 0.3$$

$$\gamma: a = 0.3 + \frac{7}{9}$$

98% containment in 3 tmax + 5

For example, 20 X_0 for 10 GeV electrons in copper

Hadronic Shower Energy Loss

- Ionization
- Hadronic cascades
- Electromagnetic showers ($e^{\pm}$, γ, π^0)
- Neutrons with nuclear-binding energies (MeV)
- Nuclear fission
- Photons from nuclear de-excitation
- ν's and μ's from π and K decays

Many of these processes provide little or no observable signal. They represent a variety of sensitivity fractions. They also take place on a variety of time scales. The contributions vary with energy and with the types of materials used for absorber and active media.

One important consequence is that the sampling fraction for hadrons is lower than that for electrons and photons, unless one takes specific countermeasures.

Hadronic Showers

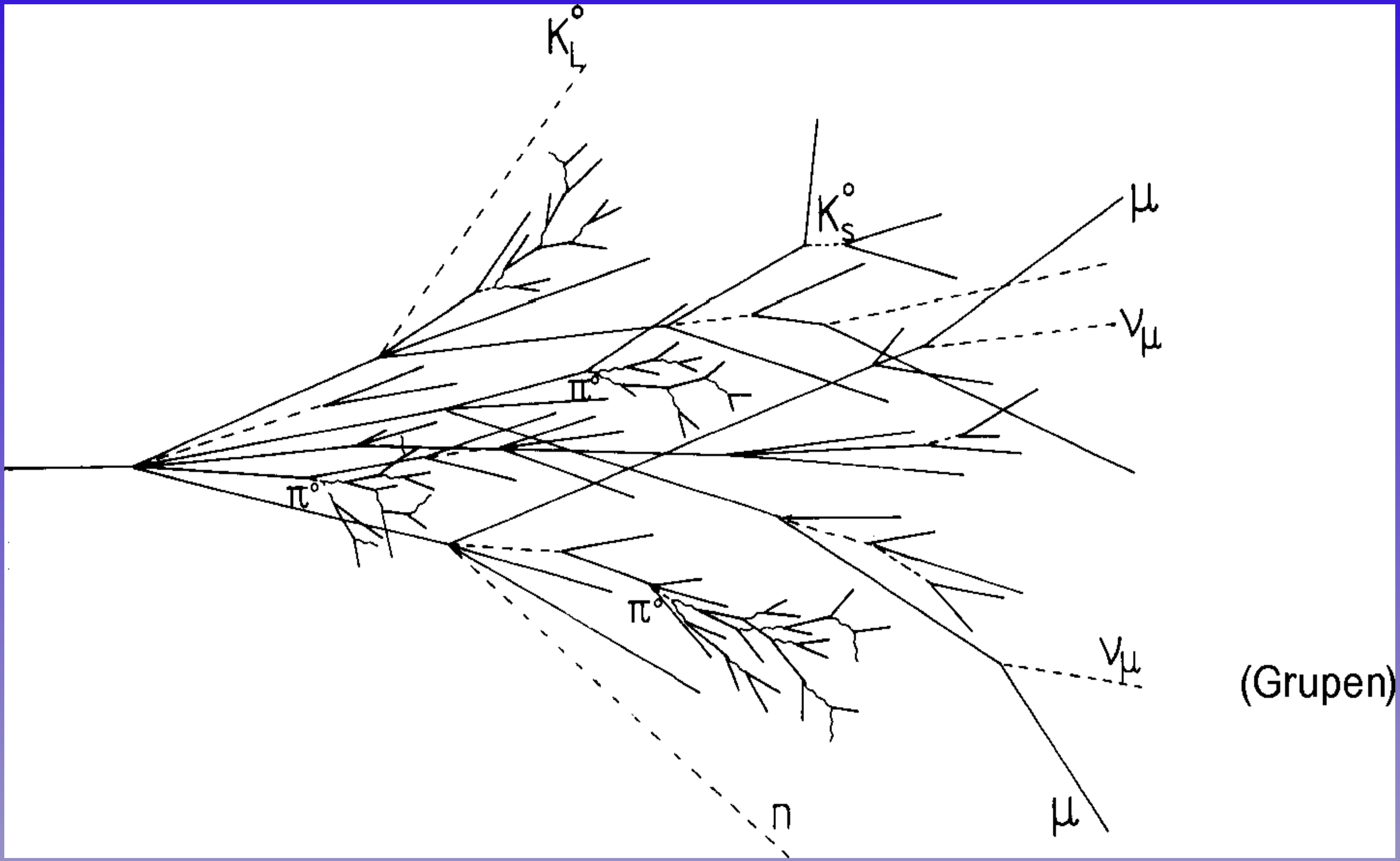

Hadron Containment

$$\lambda_I = \frac{A}{N_A}\frac{1}{\sigma}$$

$\sigma_{\mathrm{pp}} = 40$ mb (energy dependence very weak)

$\sigma_{\mathrm{pA}} \propto A^{0.71}$ (shadowing)

	σ_I (barn)	λ_I(g/cm^2)	L_I (cm)
Fe	0.7	132	17
Pb	1.8	194	17
U	2.0	199	10

$t_{max} = 0.2 \ln E + 0.7$ (E in GeV)

Homogeneous active calorimeters impractical

Note that e^{-6}=0.2%
2 in a thousand hadrons pass through
6 interaction lengths without interacting!

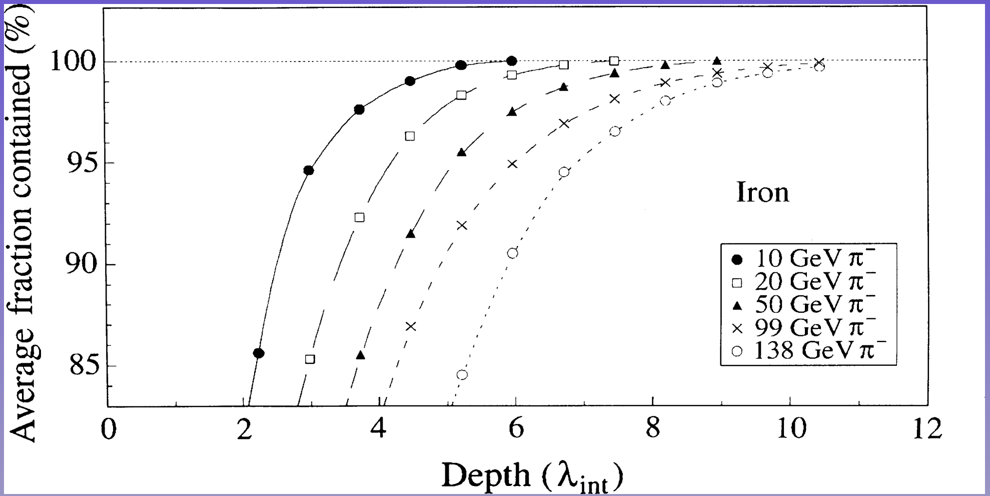

EM Fraction of Hadron Showers

Assume 1/3 of each generation is π^0's and the number of generations increases geometrically with the initial energy E. Then, if the energy to produce one π^0 is E_0, one may expect a scaling law:

$$f_{em} = 1 - (E/E_0)^{(k-1)}$$

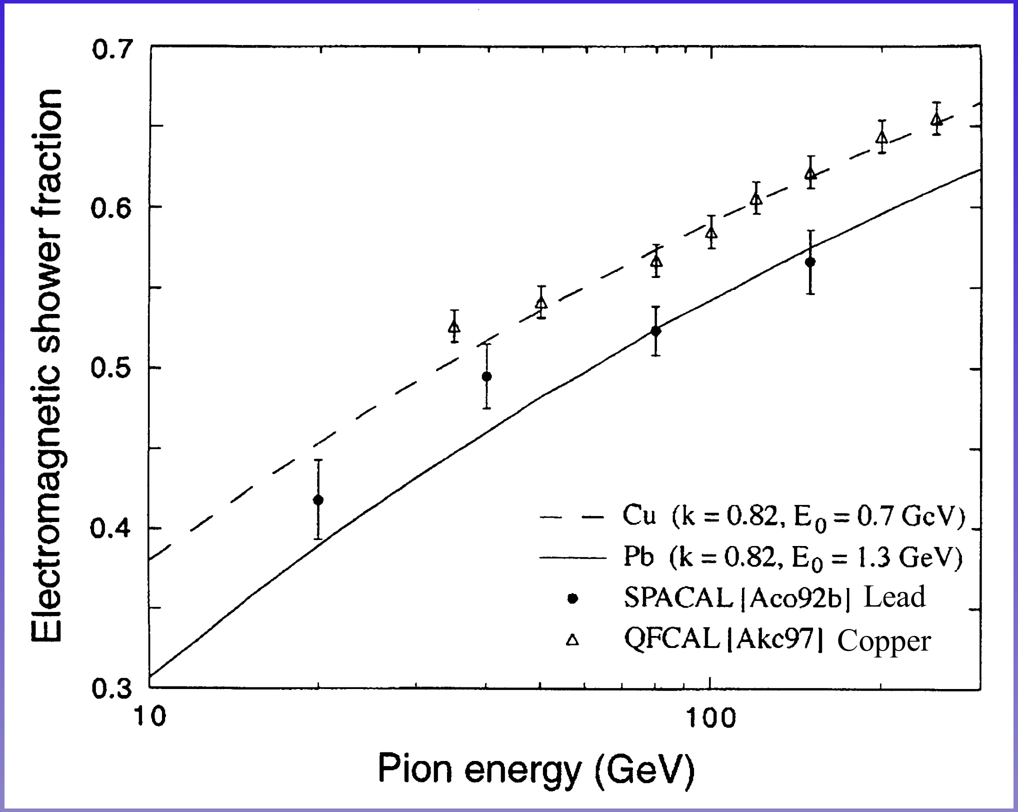

(ref: Wigmans/Gabriel)

Consequences of Differing Sampling Fractions f_{EM} and f_H

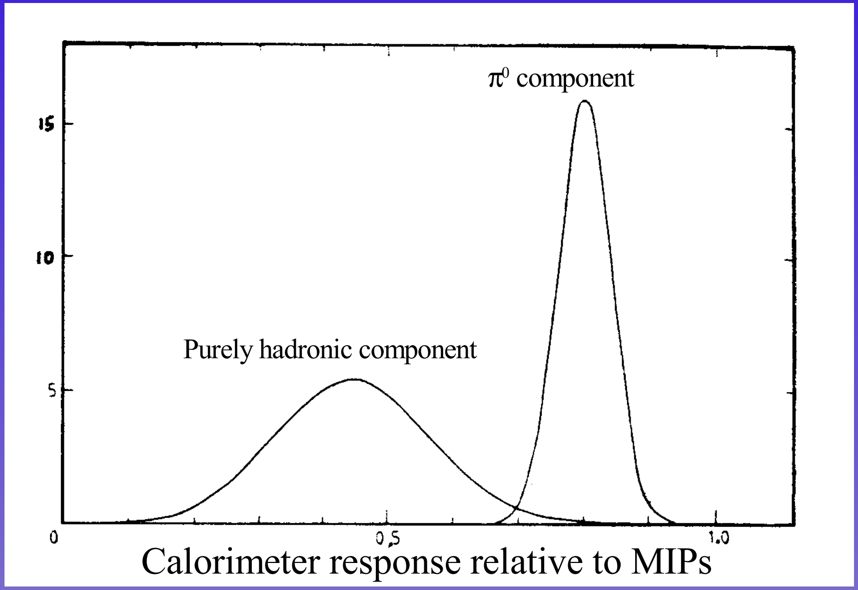

- Signal fluctuations are not gaussian
- Fluctuations in EM part affect overall resolution
- Signal is not proportional to E
- Ratio of signal for electrons and hadrons depends on energy
- Relative resolution does not scale with $E^{-1/2}$

Time Development of Hadronic Showers

The energy deposition proceeds on a variety of time scales for hadronic showers as well, unlike electromagntic showers.

This results in more complicated considerations for the choices of active media readout technology.

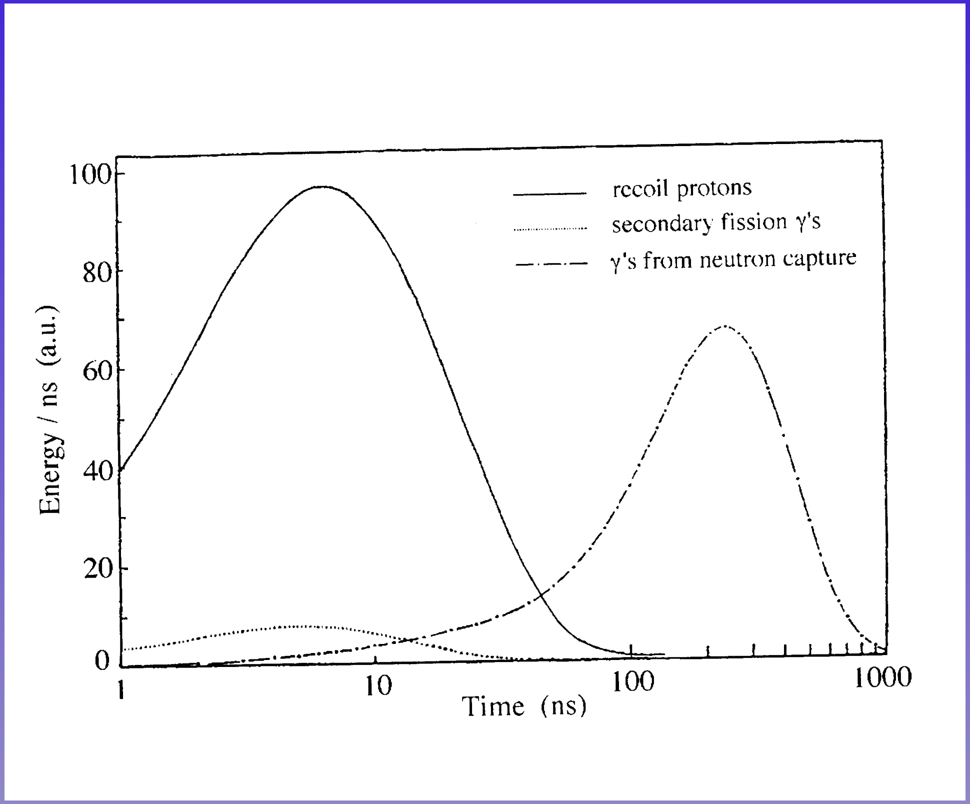

Shower Leakage

The various components of hadronic showers are contained with varying levels of success. Leakage processes which scale with the initial energy generally contribute an energy-independent term in the energy measurement resolution, reducing the effectiveness of the intrinsic statistical nature of the showers and reduce the maximum energy for which a certain level of accuracy is obtained.

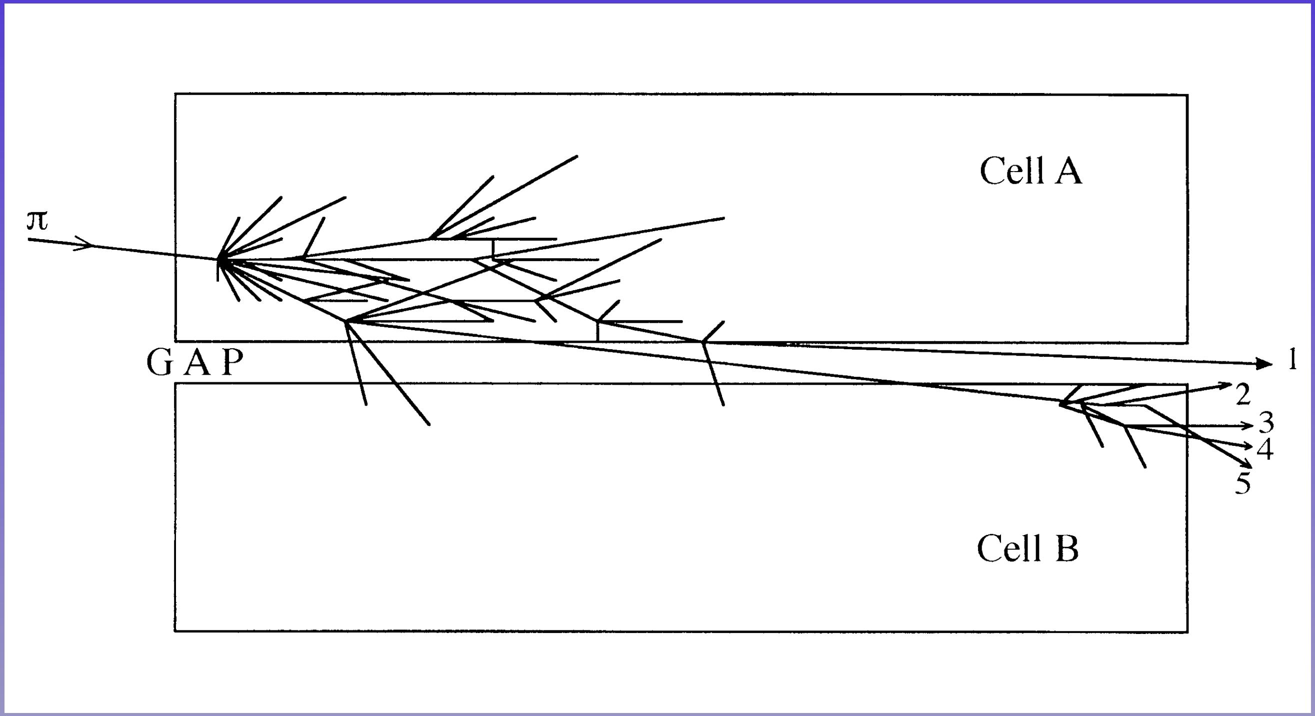

End of Section
on
Physical Processes

Muons

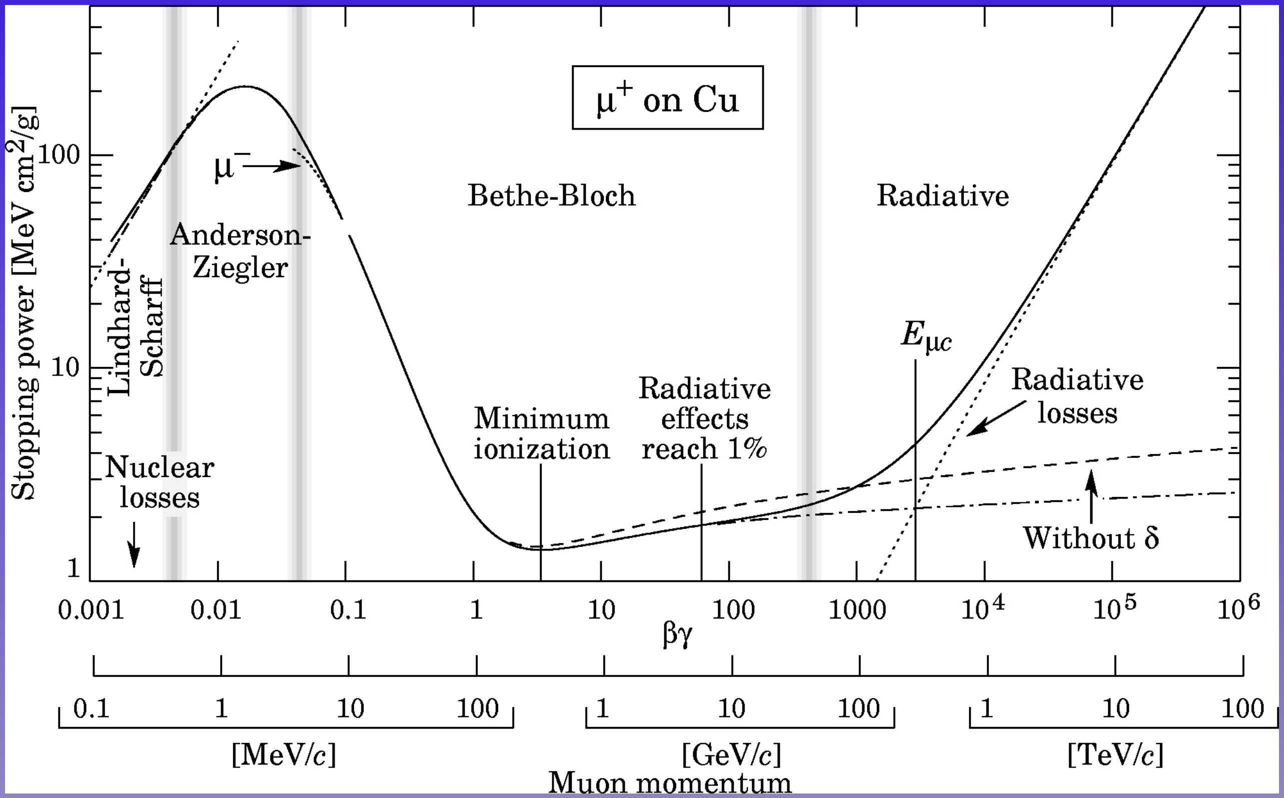

μ^+ on Cu
Stopping power [MeV cm^2/g]
100
10
1
μ^-
Anderson-
Ziegler
Lindhard-
Scharff
Nuclear
losses
Bethe-Bloch
Radiative
Minimum
ionization
Radiative
effects
reach 1%
$E_{\mu c}$
Radiative
losses
Without δ
0.001
0.01
0.1
1
10
100
1000
10^4
10^5
10^6
$\beta\gamma$
0.1
1
10
100
1
10
100
1
10
100
[MeV/c]
[GeV/c]
[TeV/c]
Muon momentum

Physikzentrum Bad Honnef